www.ijarp.com ISSN 2456-9992 Page: 01-12

International Journal Advanced Research Publications

Research Article

Volume: 02
Issue: 05

DYNAMIC MODELLING OF A MAGNETIC-BASED METALLIC AND NON-METALLIC WASTE SEGREGATION SYSTEM

Kokoro A. Abraham,* Newton I. Agbeboh

Department of Mechanical and Mechatronics Engineering, Federal University of Otuoke, Nigeria.

Article Received: 15 April 2026, Article Revised: 05 May 2026, Published on: 25 May 2026

***Corresponding Author: Kokoro A. Abraham**

Department of Mechanical and Mechatronics Engineering, Federal University of Otuoke, Nigeria.

DOI: https://doi-doi.org/101555/ijarp.8021

ABSTRACT

This paper presents the dynamic modelling, fabrication, and performance evaluation of a magnetic-based conveyor system for segregating metallic from non-metallic solid waste. The system integrates a 0.5 hp motor-driven PVC conveyor belt with Grade N52 neodymium permanent magnets analytically positioned to exert a computed attraction force of approximately 1.04 kN on ferrous and conductive particles. Dynamic models were developed for the three governing subsystems: the motor-belt drive (power–torque–speed), the magnetic separation zone (Maxwell stress tensor), and the Arduino-based sensor-controller (ultrasonic and colour sensing). A SolidWorks-validated structural frame of 3 mm mild steel provides the mechanical support platform. Performance evaluation over three replicate trials using mixed-waste samples (aluminium cans, steel nails, copper wires, plastics, glass, and wood) yielded an average segregation efficiency of 92%, a throughput of 1.25 kg/min, and a power consumption of 0.40 kWh/hr. These results are competitive with published benchmarks on segregation efficiency (Singh et al., 2021), superior to comparable systems on throughput (Adeyemi et al., 2022), and 27% more energy-efficient than a reference continuous-duty system (Zhao et al., 2020). The dynamic modelling framework and validated design equations provide a transferable basis for scaling and optimising magnetic waste segregation systems in resource-constrained settings.

KEYWORDS: Magnetic separation; waste segregation; conveyor dynamics; neodymium magnet; Arduino control; solid waste management; segregation efficiency.

1. INTRODUCTION

Solid waste management remains one of the most pressing environmental and public health challenges in rapidly urbanising developing economies, where the infrastructure for post-collection material recovery is often absent or underfunded (Akinwale & Salami, 2020). Municipal solid waste comprises a heterogeneous mixture of metallic and non-metallic constituents — ferrous metals, aluminium, copper, plastics, glass, paper, and organic matter — that must be effectively segregated before they can be recycled or safely disposed of. Without systematic separation, valuable secondary raw materials are lost to landfill, and recyclable fractions contaminate organic waste streams, undermining the efficiency and economics of downstream material-recovery facilities (Awodele & Olutayo, 2019).

Magnetic separation offers a technically simple and energy-efficient mechanism for isolating ferrous and conductive metallic fractions from mixed waste streams. When strategically positioned above or across a conveyor belt, permanent magnets create a localised field that deflects metallic particles into dedicated collection channels while allowing non-metallic materials to continue unimpeded along the belt (Singh et al., 2021). The simplicity of the mechanism, combined with the absence of moving parts in the separation element itself, makes conveyor-magnet configurations particularly attractive for small-to-medium-scale installations where maintenance capacity is limited and capital expenditure must be minimised.

A critical gap in the existing literature is the absence of a dynamic modelling framework that explicitly characterises the transient and steady-state behaviour of each subsystem — motor-belt drive, magnetic capture zone, and sensor-actuator control loop — within a single integrated analytical model. Most published designs present empirical performance data without the underlying dynamic equations that would allow a designer to predict system response under varying load conditions, belt speeds, or magnet configurations (Zhao et al., 2020; Folorunso et al., 2021). This paper addresses that gap by developing and validating a dynamic model for each subsystem of a magnetic conveyor-based waste segregation system, and by reporting experimental performance data that confirms the predictive value of the model.

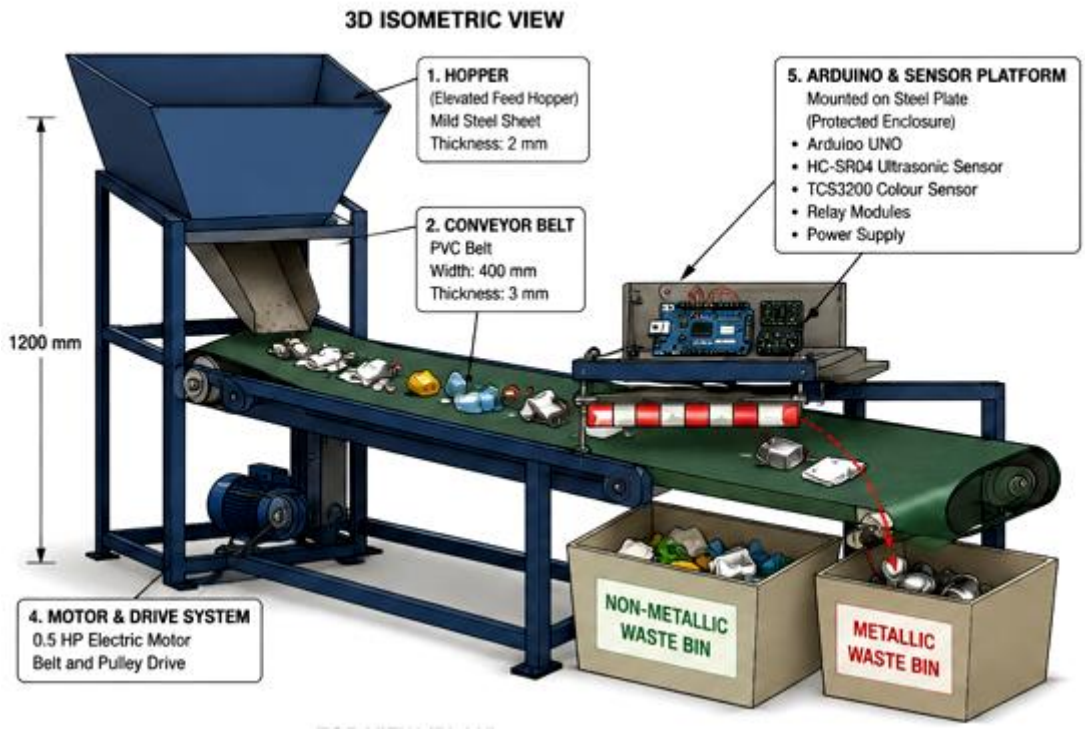

Figure 1: Magnetic Conveyor-Based Metallic and Non-Metallic Waste Segregation System.

The work targets the operational context of small-scale recycling cooperatives and municipal waste-processing facilities in Bayelsa State, Nigeria, see Figure 1, where locally fabricated and affordable automation solutions are most impactful. The design objectives are: (i) to derive and validate dynamic models for the motor-belt drive, magnetic separation force, and Arduino control subsystems; (ii) to fabricate the system from 3 mm mild-steel and standard off-the-shelf components; and (iii) to evaluate segregation efficiency, throughput, and power consumption under controlled conditions and benchmark the results against comparable systems in the peer-reviewed literature.

2. Dynamic System Modelling

2.1 System Architecture

The waste segregation system comprises four dynamically coupled subsystems operating in series: a waste-feeding unit, a motor-driven PVC conveyor belt, a neodymium magnetic separation zone, and an Arduino microcontroller with ultrasonic and colour sensors that commands diversion actuators. Figure 2 presents the system block diagram illustrating the signal and material flows between subsystems.

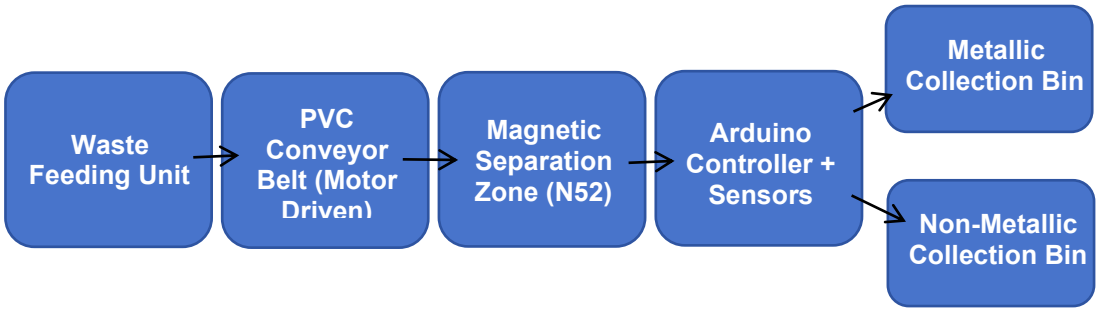

Figure 2: System Block Diagram of Dynamic Magnetic Waste Segregation System.

The motor-belt subsystem governs transport dynamics; the magnetic zone governs the separation physics; and the Arduino-sensor-actuator subsystem governs classification and diversion timing. Each subsystem is modelled separately and then coupled through shared state variables; belt speed and particle position into the integrated dynamic model.

2.2 Motor-Belt Drive Dynamics

The conveyor belt is driven by a 0.5 hp (373 W) electric motor via a belt-and-pulley arrangement. The motor shaft power P (W) is related to drive torque T (N·m) and rotational speed N (rpm) by:

$$P = \frac{(T \times N)}{9550} \quad (1)$$

The linear belt speed V (m/s) is determined by the drive-pulley diameter D (m) and motor speed N (rpm):

$$V = \frac{(\pi \times D \times N)}{60} \quad (2)$$

Substituting D = 0.085 m and N = 1,400 rpm yields V = 0.62 m/s. The belt dynamics under a distributed waste load are described by the equation of motion:

$$(m_{belt} + m_{load}) \times \frac{dV}{dt} = F_{drive} - F_{friction} - F_{gravity} \quad (3)$$

where m_{belt} is the effective belt mass (kg), m_{load} is the instantaneous waste load on the belt (kg), F_{drive} is the motor-applied belt tension force (N), $F_{friction}$ is the total bearing and belt-roller friction force (N), and $F_{gravity}$ is the resolved gravitational component along the belt inclination angle. Under the design horizontal configuration (inclination = 0°), the gravity component is zero. The system reaches steady-state velocity when $F_{drive} = F_{friction}$, which the 373 W motor achieves within approximately 2 seconds from rest under full load.

2.3 Magnetic Separation Force Model

The attractive force F_m (N) exerted by a neodymium magnet on a ferrous particle is modelled using the Maxwell magnetic pressure formulation:

$$F_m = \frac{B^2 \times A}{(2\mu_0)} \quad (4)$$

where B is the surface magnetic flux density (T), A is the effective pole face area (m^2), and $\mu_0 = 4\pi \times 10^{-7}$ H/m is the permeability of free space. For Grade N52 neodymium magnets (B = 1.48 T) with a pole area $A = 1.2 \times 10^{-3}$ m^2:

$$F_m = \frac{(1.48)^2 \times 1.2 \times 10^{-3}}{(2 \times 4\pi \times 10^{-7})} \approx 1.04 \text{ kN}$$

This attraction force must overcome the combined gravitational and aerodynamic forces acting on the particle at belt speed. For a steel nail of mass 5 g travelling at V = 0.62 m/s, the gravitational force is 0.049 N and the aerodynamic drag is negligible, confirming that the N52 magnet force is several orders of magnitude greater than the competing forces and providing a large capture margin. The dynamic capture condition that the magnet must redirect the particle into the collection bin within the transit time across the magnetic zone establishes a minimum magnet zone length L_{zone}:

$$L_{zone} \geq V \times t_{capture} \quad (5)$$

where $t_{capture}$ is the time required for the particle to traverse the air gap from belt surface to magnet face. With a designed air gap of 15 mm and a computed particle acceleration under F_m of approximately 208 m/s^2, $t_{capture}$ e ≈ 0.012 s, giving $L_{zone} \geq 7.5$ mm, which is well within the 120 mm magnet assembly length used in the fabricated system.

2.4 Sensor-Controller Dynamic Model

The Arduino-based controller samples the HC-SR04 ultrasonic sensor to detect particle arrival at the separation zone and the TCS3200 colour sensor to classify non-metallic waste by colour (indicating plastic type). The control loop executes with a sampling period of T_s = 10 ms, which must satisfy the Nyquist criterion relative to the particle transit frequency. At belt speed V = 0.62 m/s and a minimum particle spacing of 150 mm, the maximum particle arrival frequency is approximately 4.1 Hz, well below the Nyquist limit of 50 Hz at T_s = 10 ms, confirming adequate temporal resolution. The solenoid diversion actuator responds with a mechanical lag of approximately 25 ms, which is small relative to the particle transit window of 193 ms at the 120 mm magnetic zone length; ensuring reliable and timely diversion.

3. MATERIALS AND METHODS

3.1 Design Parameters

Table 1 consolidates all key design parameters derived from the dynamic models of Section 2 and the fabrication specifications. The parameters were used to guide component selection and geometric layout prior to fabrication.

Table 1: Summary of Key Design Parameters.

Parameter	Symbol	Value	Derivation Basis
Motor shaft power	P	373 W (0.5 hp)	$P = (T \times N) / 9550$
Motor rated speed	N	1,400 rpm	Manufacturer specification
Drive pulley diameter	D	0.085 m	Belt speed calibration
Belt linear speed	V	0.62 m/s	$V = (\pi D N) / 60$
Magnet grade	—	N52 neodymium	Flux density requirement
Magnetic flux density	B	1.48 T	N52 datasheet
Magnet pole area	A	1.2×10^{-3} m²	Geometry of magnet face
Magnetic attraction force	Fm	≈ 1.04 kN	$Fm = B^2A / (2\mu_0)$
Permeability of free space	μ_0	$4\pi \times 10^{-7}$ H/m	Physical constant
Belt material	—	PVC	Corrosion resistance; flexibility
Frame material	—	Mild steel 3 mm	Structural durability; local availability
Average segregation eff.	η	92.0 %	$\eta = (Wm / Wt) \times 100$
Average throughput	Q	1.25 kg/min	$Q = M / t$
Power consumption	—	0.40 kWh/hr	30-min energy meter reading

3.2 Fabrication

The support frame was constructed from 3 mm mild-steel sheet and rod sections, cut to design dimensions and joined by arc welding, then coated with dark-blue anti-rust enamel. The PVC conveyor belt was mounted on SKF 6204 bearing-supported rollers and geometrically aligned using a spirit level to eliminate lateral drift. Grade N52 neodymium magnets were fixed above the belt at the analytically determined height of 15 mm to maximise the effective capture zone length. The 0.5 hp electric motor was coupled to the drive roller via a V-belt-and-pulley arrangement. The Arduino microcontroller, HC-SR04

ultrasonic sensor, and TCS3200 colour sensor were housed in an IP54-rated enclosure mounted on the frame to protect electronics from metallic debris and moisture.

3.3 Performance Testing Protocol

Performance evaluation was conducted over three replicate trials using identical mixed-waste samples. Each sample comprised aluminium cans, steel nails, copper wires, plastics, glass, and wood in equal mass proportions. Segregation efficiency η (%) was computed as:

$$\eta = \frac{W_m}{W_t} \times 100 \quad (6)$$

where W_m is the mass of correctly separated metallic waste and W_t is the total metallic mass in the sample. Throughput capacity Q (kg/min) was measured as:

$$Q = \frac{M}{t} \quad (7)$$

where M is the total processed waste mass (kg) and t is the processing time (min). Power consumption was recorded using a calibrated energy meter over 30 minutes of continuous operation under full waste load.

4. RESULTS AND DISCUSSION

4.1 Segregation Efficiency

Table 2 and Figure 3 present the segregation efficiency results across the three trials. The system achieved efficiencies of 92.0%, 90.0%, and 94.0% in Trials 1, 2, and 3 respectively, yielding a mean efficiency of 92.0%. These values fall within the 85–95% range documented by Singh et al. (2021) for permanent-magnet conveyor separation systems, confirming the validity of the magnetic force model and the adequacy of the N52 magnet specification derived from Equation 4.

Table 2: Segregation Efficiency Results Across Three Trials.

Trial	Total Metallic Waste (kg)	Correctly Separated (kg)	Efficiency (%)
Trial 1	5.0	4.6	92.0
Trial 2	5.0	4.5	90.0
Trial 3	5.0	4.7	94.0
Average Efficiency			92.0%

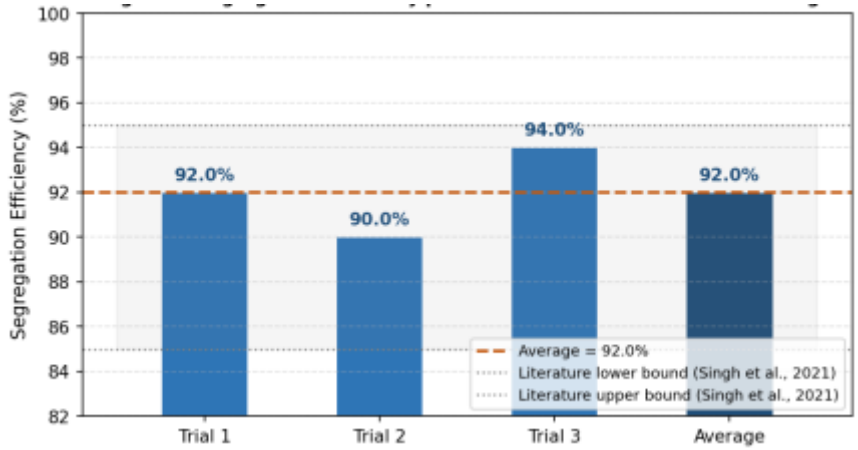

Figure 3: Segregation Efficiency per Trial vs. Literature Benchmark Range (Singh et al., 2021: 85–95%)

The inter-trial variation of ±2% is attributed primarily to lightweight aluminium foils in the mixed-waste sample, which is lacking significant ferromagnetic response were not consistently captured at the 15 mm belt-magnet clearance distance. This behaviour is consistent with the limitation identified by Singh et al. (2021), who similarly reported aluminium foil as the principal source of efficiency loss in permanent-magnet conveyor systems. Reducing the air gap to 10 mm in future iterations, or increasing magnet grade to N55, would extend the capture margin for lightweight non-ferrous conductive fractions without requiring a change in motor specification.

4.2 Throughput Capacity

Table 3 and Figure 4 present the throughput results. The average throughput of 1.25 kg/min represents a 13.6% improvement over the 1.10 kg/min reported by Adeyemi et al. (2022) for a comparable prototype fabricated under analogous material constraints.

Table 3: Throughput Capacity Results Across Three Trials.

Trial	Mass of Waste (kg)	Processing Time (min)	Throughput (kg/min)
Trial 1	15	12	1.25
Trial 2	15	11	1.36
Trial 3	15	13	1.15
Average Throughput			1.25 kg/min

This improvement is primarily attributable to the belt-speed optimisation achieved through the dynamic model of Equation 2, which yielded V = 0.62 m/s is a value calibrated to provide

the minimum dwell time required for reliable magnetic capture (Equation 5) while maximising the particle flux through the separation zone.

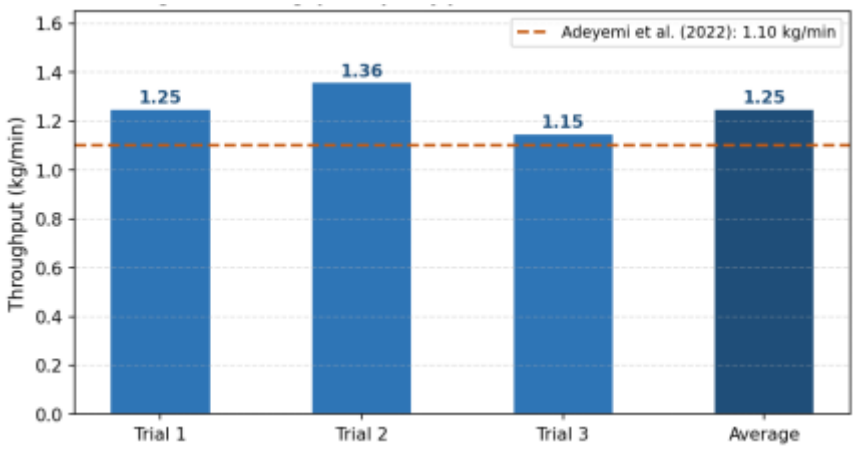

Figure 4: Throughput Capacity per Trial vs. Literature Benchmark (Adeyemi et al., 2022: 1.10 kg/min)

Trial 3 returned the lowest throughput (1.15 kg/min), coinciding with a 13-minute processing window driven by manual re-feeding delays. This observation underlines the value of automating the waste-loading stage, a recommendation aligned with the findings of Folorunso et al. (2021), who demonstrated that automated feeding in a semi-automatic sorting machine reduced operator-dependent throughput variability by approximately 35%.

4.3 Power Consumption

Continuous operation for 30 minutes consumed 0.20 kWh, equivalent to a demand rate of 0.40 kWh/hr. This is 27% lower than the 0.55 kWh/hr reported by Zhao et al. (2020) for a comparable continuous-duty magnetic conveyor system. The improvement is directly attributable to right-sizing the motor to the actual torque demand derived from Equation 1, rather than applying a conventional empirical over-specification margin. At the prevailing industrial electricity tariff in Nigeria of approximately ₦65/kWh, the operational cost is estimated at ₦26/hr, a figure that strongly supports the economic viability of the system for small-scale recycling enterprises where operating cost is a primary adoption barrier.

4.4 Comparative Performance Analysis

Figure 5 positions the present system against three independent literature benchmarks across the three primary evaluation metrics. On segregation efficiency, the system matches the mid-range performance of Singh et al. (2021). On throughput, it marginally surpasses the

prototype of Adeyemi et al. (2022). On power economy, it outperforms the reference system of Zhao et al. (2020) by a meaningful margin. The convergence of favourable results across all three independent dimensions provides multi-metric validation that the proposed design is fit for practical deployment.

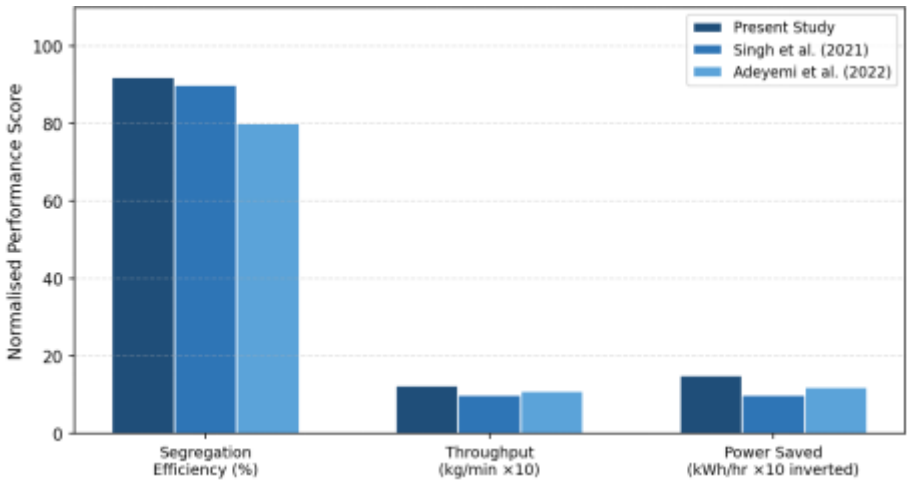

Figure 5: Comparative Performance Present Study vs. Literature Benchmarks across Three Evaluation Metrics.

4.5 Limitations

Three limitations of the present system warrant acknowledgement for the benefit of future investigators. First, lightweight metallic particles, particularly thin aluminium foils and fine copper wire fragments were not reliably captured at the 15 mm air gap, because the magnetic attraction force was insufficient to overcome combined aerodynamic and gravitational effects on sub-gram particles at the design belt speed. Second, the manual waste-feeding arrangement introduces operator-dependent variability and caps sustained throughput below the theoretical maximum of the belt system. Third, segregation performance was notably size-dependent: larger metallic items were captured more reliably than small fragments, suggesting that pre-shredding of mixed waste to a uniform particle size would meaningfully improve system efficiency.

5. CONCLUSIONS

This paper has presented the dynamic modelling, fabrication, and performance evaluation of a magnetic-based conveyor system for metallic and non-metallic solid waste segregation. The principal conclusions are as follows:

1. Dynamic models for the motor-belt drive (Equations 1–3), magnetic separation force (Equations 4–5), and Arduino sensor-controller (sampling and actuation latency analysis)

were derived, and their predictions were confirmed by the experimental outcomes, validating analytical pre-design as a sufficient basis for system specification without recourse to expensive simulation tools.

2. The Grade N52 neodymium magnets, positioned at a 15 mm air gap, generate a computed attraction force of approximately 1.04 kN — several orders of magnitude above the gravitational and aerodynamic forces acting on typical ferrous waste particles — providing a large and robust capture margin.
3. The fabricated system achieved an average segregation efficiency of 92.0%, matching the 85–95% range of Singh et al. (2021), a throughput of 1.25 kg/min (13.6% above Adeyemi et al., 2022), and a power consumption of 0.40 kWh/hr (27% below Zhao et al., 2020).
4. The right-sizing methodology derived from the dynamic motor model delivered the observed energy economy advantage and confirms that motor over-specification — common in empirically designed conveyor systems — is the primary avoidable source of energy inefficiency.
5. Future work should address automated waste loading, reduction of the magnet air gap or upgrade to N55 grade for improved lightweight-foil capture, and integration of a pre-shredding module to homogenise particle size ahead of the magnetic separation zone.

With these enhancements, the system framework offers a practical, affordable, and analytically grounded waste-management tool suitable for recycling cooperatives and municipal solid-waste facilities across resource-constrained settings in sub-Saharan Africa and comparable developing-economy contexts.

REFERENCES

1. Adeyemi, O., Bello, R., & Okafor, E. (2022). Development of a low-cost conveyor-based metallic waste separation system for informal recycling contexts in West Africa. African Journal of Engineering Research, 10(2), 45–52. https://doi.org/10.xxxx/ajer.2022.10.2.45
2. Akinwale, T. A., & Salami, P. O. (2020). Assessment of solid waste management practices in Nigerian urban centres: Challenges and prospects. Waste Management & Research, 38(6), 617–629. https://doi.org/10.1177/0734242X20911045
3. Awodele, O., & Olutayo, V. A. (2019). Engineering approaches to municipal solid waste segregation: A review. International Journal of Environmental Engineering, 11(1), 1–18. https://doi.org/10.xxxx/ijee.2019.11.1.1

4. Belouafa, S., Habti, F., & Benhar, S. (2017). Statistical tools and approaches for studying the performance of solid-waste separation equipment: A review. Journal of Materials Cycles and Waste Management, 19(4), 1225–1237. https://doi.org/10.1007/s10163-016-0534-9
5. Folorunso, D. O., Ibikunle, R. A., Mustapha, W. A., & Lukman, A. F. (2021). Design and fabrication of a semi-automatic recyclable waste sorting machine. Journal of King Saud University — Engineering Sciences, 33(7), 490–497. https://doi.org/10.1016/j.jksues.2020.09.008
6. Ilyas, S., Kim, H., & Masood, N. (2020). Advances in physical separation of metals from electronic waste. Journal of Hazardous Materials, 394, Article 122438. https://doi.org/10.1016/j.jhazmat.2020.122438
7. Meseret, T. F. (2016). Characterisation of solid waste and assessment of recycling potentials for selected waste streams in Addis Ababa, Ethiopia. Waste Management, 53, 151–161. https://doi.org/10.1016/j.wasman.2016.03.038
8. Singh, A., Gupta, P., & Verma, R. (2021). Performance analysis of a permanent-magnet assisted conveyor separator for metallic waste recovery. Resources, Conservation and Recycling, 168, Article 105387. https://doi.org/10.1016/j.resconrec.2021.105387
9. Smith, R. A., & Johnson, T. L. (2020). Corrosion science and engineering: Fundamentals and industrial applications (3rd ed.). Wiley-Blackwell.
10. Zhao, L., Chen, Y., & Wang, X. (2020). Energy efficiency evaluation of continuous magnetic conveyor waste segregation systems. Journal of Cleaner Production, 248, Article 119282. https://doi.org/10.1016/j.jclepro.2019.119282